



## Polymerization of acrylamide inverse microemulsion initiated directly by UV radiation

Long Xie,<sup>1,2\*</sup> Ziqiang Shao,<sup>2</sup> Huiqing Wang,<sup>2</sup> Shaoyi Lv<sup>2</sup>

<sup>1\*</sup>College of Chemical Engineering and Environment, North University of China, Taiyuan 030051, P. R. China; fax: +8601068941797; e-mail: nilong1976@163.com

<sup>2</sup>School of Material Science and Engineering, Beijing Institute of Technology, Beijing 100081, P. R. China; fax: +8601068941797; e-mail: shaoziqiang@263.net

(Received: 30 October, 2010; published: 15 August, 2011)

**Abstract:** Combining the microemulsion polymerization with UV direct initiation, an efficient method for polymerization of AM with high polymerization rate and conversion, low polymerization temperature, high purity of product and simple radiation equipment was developed. In the absence of initiator and under UV radiation, the polymerizations of AM inverse microemulsion system with high monomer content and low emulsifier content were successfully accomplished at low temperature (24~30 °C) and PAM with high purity and high limiting viscosity  $[\eta]$  was obtained. The polymerization rate was fast and the conversion reached to higher than 85% in 30 minutes. Based on the abundant experimental results, the reasonable polymerization mechanisms were proposed as follows: the AM participated in the initiation reaction and the main initiation locus was the emulsifier layer.  $R_p$  and  $[\eta]$  were weakly influenced by temperature due to the low apparent activation energy of the reaction ( $E_a = 12.98$  kJ/mol). The polymerization kinetics of  $R_p$  was expressed as the following:  $R_p = [I_{UV}]^{0.4972} [M]^{1.5048} [E]^{-0.5731}$ . The  $R_p$  order with respect to  $[M]$  is equal 1.5048 which confirms the conclusion that the monomer participated in the initiation reaction.

### Introduction

Acrylamide (AM)-based polymers have been studied for its broad industrial applications, such as adhesives, efficient flocculants in different processes (e.g. paper manufacture, mineral enrichment, wastewater and potable-water treatments), and viscosity-control agents for enhancing oil recovery [1-5]. The control of solution polymerizations involving AM monomers is difficult due to the high enthalpy of polymerization ( $81.5$  kJ·mol<sup>-1</sup>) and the high viscosity of the polymers [6]. However, UV light [7, 8] and  $\gamma$ -rays [9] radiation initiation can be carried out in lower reaction temperature owing to its non-temperature dependent initiation, which benefited the control of polymerizations. Generally, the  $\gamma$ -rays radiation process can easily prepare high purity polymer without the pollution of chemical initiators, but the  $\gamma$ -rays belong to a high-energy radiation and its generation require special equipment [10]. Wada and Okada found that the  $\gamma$ -rays radiation-initiated polymers and copolymers of AM were insoluble in water at high radiation doses [11, 12].

UV radiation is a low-energy radiation and can be provided by a simple setting such as a high-pressure mercury lamp [13]. Although the UV radiation can directly initiate the polymerization of AM [13], the low initiation efficiency leads to the low polymerization rate, which limited its industrialization [14, 15]. Therefore, the photoinitiators were usually employed to enhance the initiation efficiency of UV

radiation polymerization. But the polymer purity decreased by comparing with  $\gamma$ -rays radiation initiation due to the addition of UV photoinitiators.

In order to solve all above problems, the microemulsion polymerization was employed to prepare PAM in the present work. Compared with other polymerization, the microemulsion consisted of a lot of surfactant-encapsulated water droplets suspended in a continuous oil phase [16] and every droplet may act as a polymerization reaction locus. The enormous numbers of reaction locus in the microemulsion may compensate the low efficiency of initiation by direct UV irradiation. To the best of our knowledge, in the absence of initiator, the preparation of polyacrylamide via the inverse microemulsion polymerization under UV direct radiation has not been reported yet. In this work, the AM inverse microemulsion polymerization initiated directly by UV radiation was carried out in low reaction temperature, and the polymerization mechanism was proposed on the basis of the experimental results. Furthermore, the polymerization kinetics and the influence of main factors (such as the UV irradiance, temperature and the concentration of monomer and emulsifier) on the polymerization rate  $R_p$  and on the limiting viscosity number  $[\eta]$  of PAM were investigated.

## Results and discussion

### *HLB value and formulation selection*

From an industrial viewpoint, the microemulsion should contain a high monomer content and low emulsifier content. To attain this objective, the optimum HLB value and the pseudo-ternary phase diagram were required to obtain. The optimum HLB value was selected by varying the composition of the mixture of emulsifiers. Figure 1 indicated the content of emulsifier as a function of HLB value for the different weight percentage of AM in aqueous phase at 30°C.

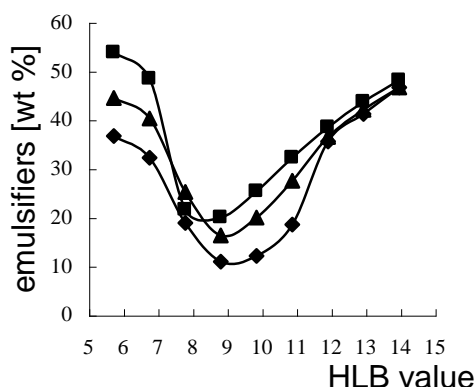


**Fig. 1.** Weight percentage of the emulsifiers required for microemulsion versus HLB of the emulsifiers blend under the different Weight percentage of AM in the aqueous phase: ■30%; ▲40%; ◆ 50%

It can be seen that the microemulsion system with the lowest emulsifier concentration was formed at HLB=8.82, which is defined as the optimum value. The pseudo-ternary phase diagram of AM microemulsion at the optimum HLB value was displayed as Figure 2, the curves indicated the transition between macroemulsion (to the right of the curves) and microemulsion (to the left of the curves). Based on the pseudo-

ternary phase diagrams, the minimum weight percentage of emulsifiers required to form a stable inverse microemulsion can be determined.

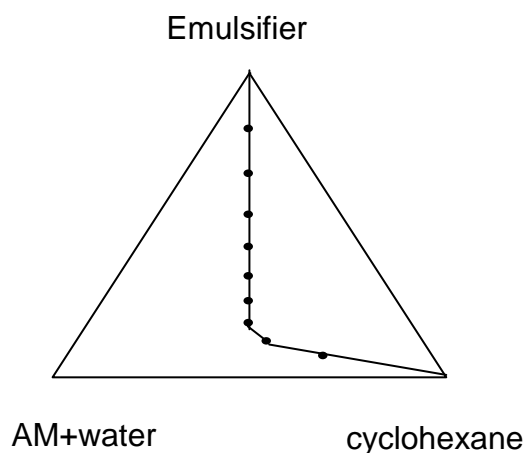


**Fig. 2.** The pseudo-ternary phase diagram of AM microemulsion at the optimum HLB value.

### *Polymerization process*

The composition of the microemulsions and the polymerization conditions in each run are shown in Table 1. The variation of polymerization rate and conversion with the reaction time is shown in Figure 3 and Figure 4.

**Tab. 1.** The formulations of polymerization.

Run	AM	Water	Cyclohexane	Span60	Tween80	Temperature	UV irradiance
R-1	6g	9g	21g	5.4g	3.6g	26°C	40.2 W/m <sup>2</sup>
R-2	6g	9g	21g	5.4g	3.6g	26°C	45.5 W/m <sup>2</sup>
R-3	6g	9g	21g	5.4g	3.6g	26°C	50.3 W/m <sup>2</sup>
R-4	6g	9g	21g	5.4g	3.6g	26°C	55.2 W/m <sup>2</sup>
R-5	7g	9g	21g	5.4g	3.6g	26°C	40.2 W/m <sup>2</sup>
R-6	5g	9g	21g	5.4g	3.6g	26°C	40.2 W/m <sup>2</sup>
R-7	4g	9g	21g	5.4g	3.6g	26°C	40.2 W/m <sup>2</sup>
R-8	6g	9g	21g	4.8g	3.2g	26°C	40.2 W/m <sup>2</sup>
R-9	6g	9g	21g	6g	4g	26°C	40.2 W/m <sup>2</sup>
R-10	6g	9g	21g	6.6g	4.4g	26°C	40.2 W/m <sup>2</sup>
R-11	6g	9g	21g	5.4g	3.6g	24°C	40.2 W/m <sup>2</sup>
R-12	6g	9g	21g	5.4g	3.6g	28°C	40.2 W/m <sup>2</sup>
R-13	6g	9g	21g	5.4g	3.6g	30°C	40.2 W/m <sup>2</sup>

It can be seen that the typical conversion–time curve (generally S-shaped) and the conversion reached to higher than 85% in 30 minutes (100% in 1 hour), which meant that the polymerization was very fast. In addition, there was no apparent constant rate period in the polymerization; this was ascribed to two opposing effects: the continual increase of polymer particle number due to continuous nucleation process [17] and continual decrease of monomer concentration at the reaction loci.

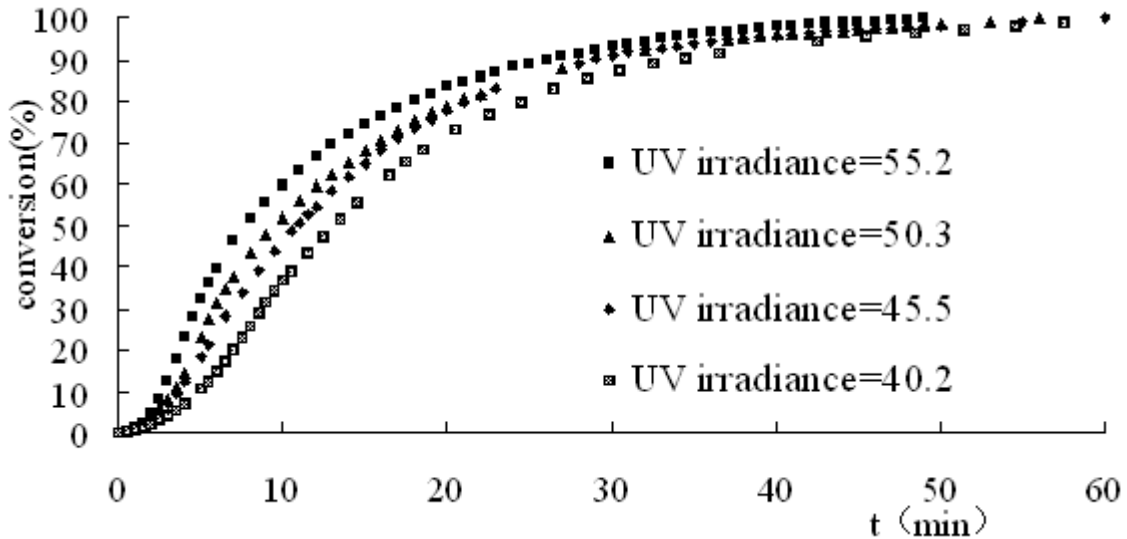


**Fig. 3.** Variation of the conversion with time under different UV irradiance ( $\text{W}/\text{m}^2$ )

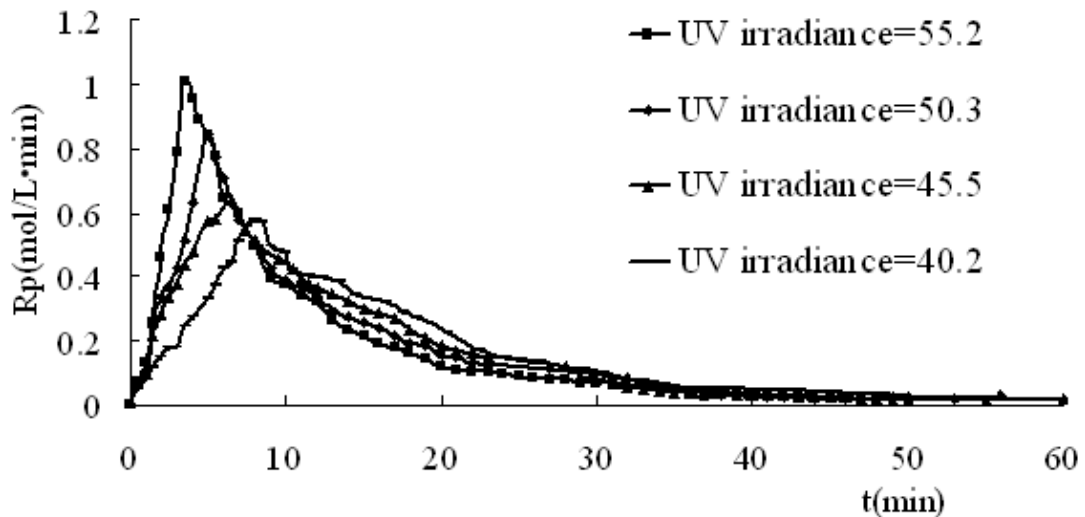


**Fig. 4.** Variation of the  $R_p$  with time under different UV irradiance ( $\text{W}/\text{m}^2$ )

### *Polymerization mechanism*

#### **-Radical formation**

In the present work the PAM was prepared in the inverse microemulsion polymerization of AM under UV radiation, without an initiator. This suggested that one component of the microemulsion system (AM monomer, emulsifiers or oil phase) participated in the initiation reaction and acted as a role of initiator. In order to confirm that the AM aqueous solution could generate the free radicals, the solution polymerization of AM aqueous solution was carried out by UV direction radiation and the PAM was obtained. Under UV radiation, the chemical bond of AM was likely to be broken to generate the free radicals [15].

#### **-Initiation locus**

As AM monomer can insert in the emulsifier layer due to its co-emulsifier ability [18], the initiation reaction may take place in emulsifier layer or the microdroplets saturated

with the aqueous solution of monomer. In our work, it was found that the transparent microemulsion became translucent just after the polymerization started, and then the transparency increased slowly with conversion. The phenomenon was similar to the microemulsion polymerization of methyl methacrylate initiated with  $\gamma$ -Ray [19]. This can be rationalized by the following initiation mechanism: the main initiation locus was the emulsifier layer, the monomer inserted in emulsifier layer was preferentially consumed after the polymerization started and lost its co-emulsifier function. As a result, the structure of microemulsion was provisionally broken and became translucent. The experimental phenomenon was consistent with the initiation mechanism, so it can be deduced that the main initiation locus was emulsifier layer.

#### Effect of UV irradiance on conversion, $R_p$ , and $[\eta]$

Figure 5 indicated the effect of UV light irradiance on the conversion,  $R_p$ , and limiting viscosity  $[\eta]$  (polymerizations were carried out as formulations listed as run1- run4 in Table 1).  $R_p$  are calculated from the linear portions of the conversions-time curves at less than 10% conversion. The correlation between the UV light irradiance  $I_{UV}$  and  $R_p$  is also displayed in Figure 5 and can be expressed as the following:  $R_p \propto [I_{UV}]^{0.4972}$ .

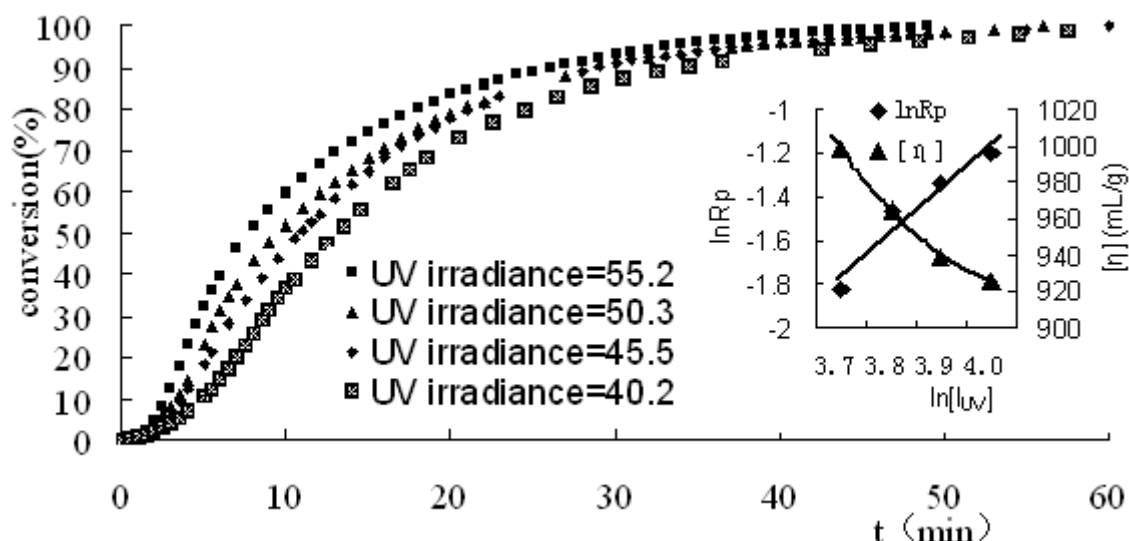


**Fig. 5.** Variations of the conversion,  $R_p$ , and  $[\eta]$  with UV irradiance ( $W/m^2$ )

It can be seen that  $R_p$  increased and  $[\eta]$  decreased as the UV irradiance increased. The results conformed to the general polymerization kinetics. As the UV irradiance increased, the rate of free-radical formation become greater. The higher rate of free radical initiation leads to faster monomer consumption and a shorter kinetic chain length. Therefore, in order to obtain PAM with high  $[\eta]$ , the appropriate UV irradiance was  $40.2 W/m^2$ .

#### Effect of monomer concentration on $R_p$ and $[\eta]$

Figure 6 indicated the effect of concentration of AM in the aqueous phase on the  $R_p$  and limiting viscosity  $[\eta]$  (polymerizations were carried out as formulations listed in run1 and run5-run7).  $R_p$  are calculated from the linear portions of the conversions-time curves at less than 10% conversion. The correlation between the monomer concentration and  $R_p$  is also displayed in Figure 6 and can be expressed as the following:  $R_p \propto [M]^{1.5048}$ . The order of  $R_p$  with respect to  $[M]$  is equal to 1.5048, near

to 3/2 in the conventional radical polymerization when the monomer participated in the initiation reaction, which confirmed that the monomer took part in the initiation reaction under UV radiation.

Both  $R_p$  and  $[\eta]$  increased when the concentration of AM in the aqueous phase increased, which is in line with the theory of free radical polymerization. In our research, as the concentration of AM in the aqueous phase is high (30%-44%), the PAM with high  $[\eta]$  (700-1100 mL/g) was obtained.

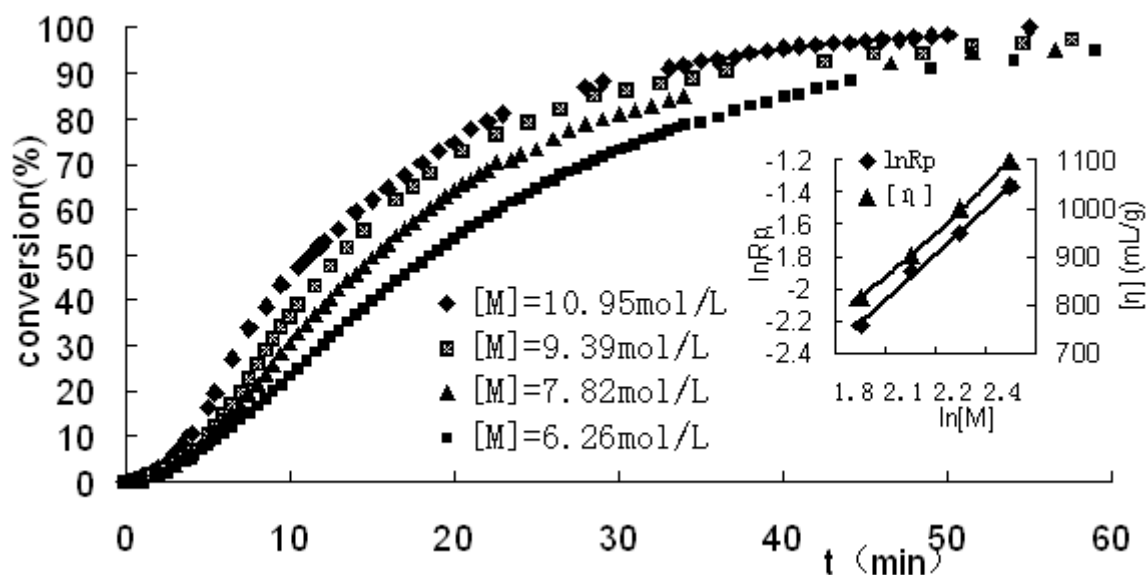


**Fig. 6.** Variations of the conversion,  $R_p$ , and  $[\eta]$  with monomer concentration.

#### *Effect of emulsifier concentration on conversion, $R_p$ , and $[\eta]$*

The variations of the  $R_p$  and  $[\eta]$  with emulsifier concentration (polymerizations were carried out as formulations listed in run1 and run8-run10) are shown in Figure 7. The correlation between the emulsifier concentration and  $R_p$  is also displayed in Figure 7 and can be expressed as the following:  $R_p = [E]^{-0.5731}$ .

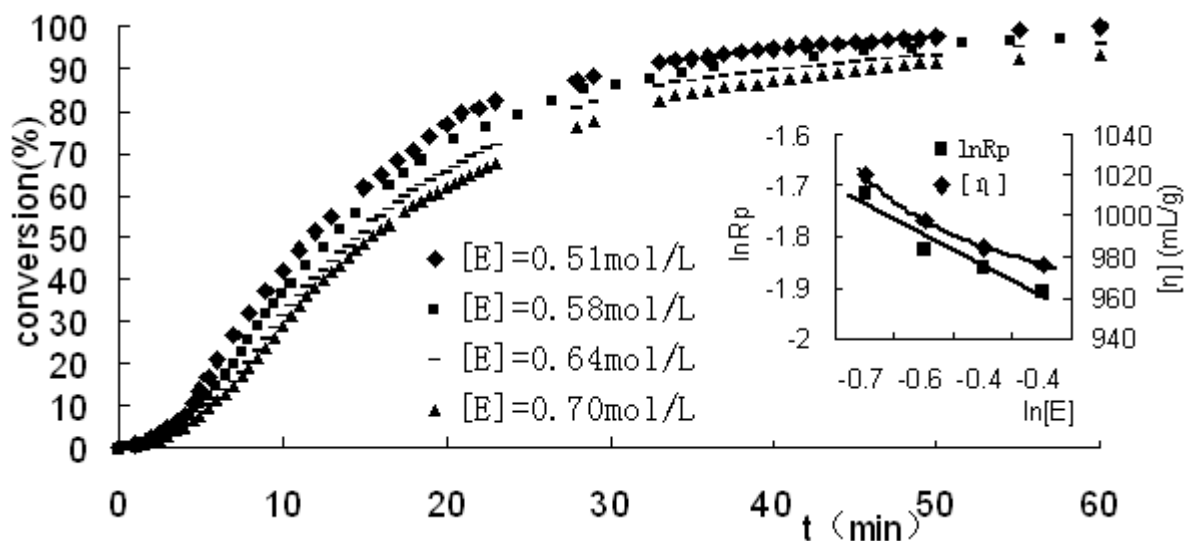


**Fig. 7.** Variations of the conversion,  $R_p$ , and  $[\eta]$  with emulsifiers concentration.

It can be seen that both  $R_p$  and  $[\eta]$  decreased when the emulsifier's concentration increased. This result can be rationalized: the main initiation loci are the emulsifier layer, the monomer concentration in the emulsifier layer is suppressed with the increase of emulsifier concentration. The decrease of monomer concentration in the initiation loci lead to the decrease of initiation rate, which caused the decrease of polymerization rate. In addition, the probability of the chain transfer reaction to emulsifier increased with increase of the emulsifier content and radicals could be generated simultaneously also on surfactant molecules. All these led to the early termination of chain radical. These effects above-mentioned resulted in the decrease of  $R_p$  and  $[\eta]$ . The order (-0.5731) of  $R_p$  in respect to  $[E]$  indicated that  $R_p$  was strongly influenced by emulsifier's concentration.

### Effect of temperature on conversion, $R_p$ , and $[\eta]$

The variations of the  $R_p$  and  $[\eta]$  with polymerization temperature when all the other variables were kept constant (polymerizations were carried out as formulations listed in run1 and run11-run13) are shown in Figure 8. It can be seen that  $R_p$  increased and  $[\eta]$  decreased when the temperature increased, but the changes were very little. As  $R_p$  was directly proportional to the reaction rate constant  $k$  ( $R_p \propto k$ ) and according to the Arrhenius equation ( $k=Ae^{(-E_a/RT)}$ ), the relationship of  $R_p$  and  $E_a$  was expressed as  $R_p \propto Ae^{(-E_a/RT)}$ . Therefore, the apparent activation energy ( $E_a$ ) can be calculated from the slope of the  $\ln(R_p)$ - $1/T$  curve. The  $E_a$  was figured out to be 12.98 kJ/mol from Figure 8. The value was smaller than that of the thermal initiation polymerization [20] ( $E_a=65.7$  kJ/mol) initiated by 2,2'-azobis(2-amidinopropane) dihydrochloride and was similar to that of the radiation-induced polymerization [21] ( $E_a=10.57$  kJ/mol) initiated by  $\gamma$ -rays. This meant that the polymerization in our research was relatively easy to implement in low temperature (lower than 30 °C) and was weakly influenced by temperature.

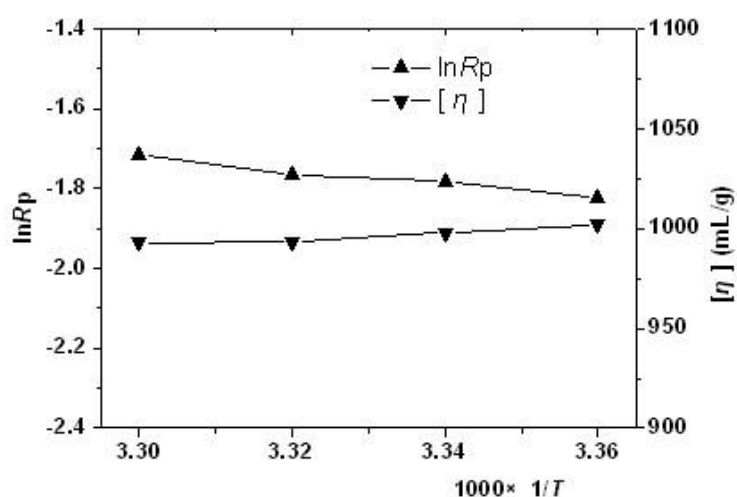


**Fig. 8.** Variations of the  $R_p$  and  $[\eta]$  with polymerization temperature

## Experimental part

### Materials

AM with a purity of 99.5 wt% was purchased from QiXian polymer Co. Ltd, China, and recrystallized twice from chloroform. Span 60 (purity  $\geq 90.0$  wt%, from J&K

Chemical Ltd, China) and Tween 80 (purity  $\geq 90.0$  wt%, from J&K Chemical Ltd, China) were used as received. Nitrogen with a purity of 99.99% was purchased from Beijing Chemical Ltd, China, and was used to eliminate the dissolved oxygen. High-pressure mercury lamp (the wavelength range, 200-400nm) was purchased from Beijing Lamp-House Ltd, China, and used as an ultraviolet light source.

### *Phase Diagram Determination*

The pseudo-ternary phase diagram consisted of monomer aqueous solution, oil phase and emulsifiers. First, the monomer aqueous solution was placed in a 25-mL vial and thermostated at 30 °C. Then, the blend of the oil phase and the mixture of emulsifiers were slowly added, drop by drop, under vigorous stirring until the turbid emulsion turned into an optically transparent microemulsion. At this moment, the conductivity of the microemulsion was close to that of cyclohexane, and this showed that the microemulsion had a globular structure, which was formed by micelles swollen with the aqueous phase. The final composition of the microemulsion was determined by weighing.

### *Inverse microemulsion polymerization of AM*

According to the inverse microemulsion domain of the pseudo-ternary phase diagram, the inverse microemulsions were prepared by mixing the required quantities of the cyclohexane, monomer aqueous solution and emulsifiers under stirring. After the formation of transparent microemulsion, the liquid was purged with nitrogen for 30 minutes and transferred into a glass reactor equipped with magnetic stirrer. Finally, without initiator added, the polymerization was carried out under the UV radiation provided by the high-pressure mercury lamp. When the reaction finished, the polymeric product was precipitated from the microemulsion by adding an excess of ethanol, the precipitated polymer was thoroughly washed with ethanol and dried. The reaction equipment was shown schematically in Figure 9.

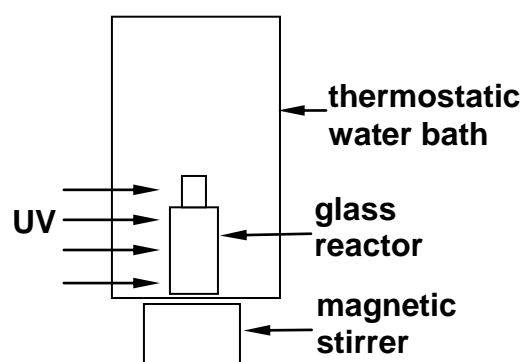


**Fig. 9.** Schematic illustration of reaction equipment

### *Characterization*

The dilatometric method has been used to determine conversion and polymerization rate as described in reference [22]. By derivation of the curves of the volume contraction ( $V_t$ ) with the polymerization time ( $t$ ), the conversion of monomers was obtained from  $V_t/V_M$ , and the polymerization rate was calculated from  $(\Delta V_t \cdot M_0)/(V_M \cdot \Delta t)$ .  $V_t$  is the volume contraction;  $V_M$  is the final volume contraction when the conversion reached 100%;  $M_0$  is the initial monomer concentration.

The limiting viscosity number  $[\eta]$  of PAM was determined in the Ubbelohde viscosity meter with 0.5 mm capillary diameter at 25 °C. PAM was dissolved in 0.1 M aqueous NaCl solution to form a clear liquid with the concentration range from 0.2 to 0.3 g/L. The limiting viscosity number  $[\eta]$  is equivalent with the viscosity mean molar mass  $M_v$  according to the following equation [18]:  $[\eta] = 9.33 \times 10^{-5} M_v^{0.75}$  (mL·g<sup>-1</sup>). The  $[\eta]$  was adopted for results and discussion in this paper.

## References

- [1] McGuire, M. J.; Addai, M. J.; Bremmell, K. E. *Colloids Surf. A* **2006**, 275, 153.
- [2] Mpofo, P.; Addai, M. J.; Ralston, J. *J. Colloid Interf. Sci.* **2004**, 271, 145.
- [3] Kurenkov, V. F.; Myagchenkov, V. A. *Polym. Plast. Technol. Eng.* **1991**, 30, 367.
- [4] Pefferkorn, E. *J. Colloid Interf. Sci.* **1999**, 216, 197.
- [5] Caskey, J. A.; Peimus, R. J. *Environ. Prog.* **1986**, 5, 98.
- [6] Renteria, M.; Munoz, M.; Ochoa, J. R. *J. Polym. Sci. Polym. Chem.* **2005**, 43, 2495.
- [7] Carver, M. T.; Candau, F.; Fitch, R. M. *J. Polym. Sci., Polym. Chem.* **1989**, 27, 2179.
- [8] Fouassier, J. P.; Loughnot, D. J.; Zuchowicz, I. *Eur. Polym. J.* **1986**, 22, 933.
- [9] Alam, M. M.; Akhtar, F.; Mina, M. F. *Polym.-Plast. Technol. Eng.* **2003**, 42, 285.
- [10] Ravve, A. "Principles of Polymer Chemistry", Plenum, New York, **1995**.
- [11] Wada, T.; Sekiya, H.; Mach, S. *J. Appl. Polym. Sci.* **1976**, 20, 3233.
- [12] Okada, T.; Ishigki, I.; Suma, T. *J. Appl. Polym. Sci.* **1979**, 24, 1713.
- [13] Siyam, T. *Des. Monomers Polym.* **2001**, 4, 107.
- [14] Moad, G.; Solomon, D. H. "The Chemistry of Radical Polymerization", 2<sup>nd</sup> edition, Elsevier, Amsterdam, **2006**.
- [15] Vollmert, B. "Polymer Chemistry", Springer, Berlin, **1973**.
- [16] Antonietti, M.; Bastem, R.; Lohmann, S. *Macromol. Chem. Phys.* **1995**, 196, 441.
- [17] Candau, F.; Leong, Y. S.; Pouyet, G. *J. Colloid Interf. Sci.* **1984**, 101, 167.
- [18] Barton, J.; Stillhammerova, M. *Angew. Makromol. Chem.* **1996**, 237, 113.
- [19] Xu, X. L.; Ge, X. W.; Zhang, Z. C. *J. Appl. Polym. Sci.* **1999**, 73, 2621.
- [20] Wu, Y. M.; Liu, Y. T.; Xu, J. *e-Polymers* **2010**, no. 078.
- [21] Ye, Q.; He, W. D.; Ge, X. W. *J. Appl. Polym. Sci.* **2002**, 86, 2567.
- [22] Barton, J.; Stillhammerova, M.; Lezovic, M. *Angew. Makromol. Chem.* **1996**, 237, 99.